Published in final edited form as:
J Cardiovasc Electrophysiol. 2012 March ; 23(3): 309–318. doi:10.1111/j.1540-8167.2011.02191.x.

Electrophysiological Mapping of Embryonic Mouse Hearts: Mechanisms for Developmental Pacemaker Switch and Internodal Conduction Pathway

Tongyin Yi, M.D.[*], **Johnson Wong, B.S.**[*], **Eric Feller**[*], **Samantha Sink, B.S.**[*], **Ouarda Taghli-lamallem, PH.D.**[*], **Jianyan Wen, M.D., PH.D.**[*], **Changsung Kim, PH.D.**[*], **Martin Fink, PH.D.**[†], **Wayne Giles, PH.D.**[‡], **Walid Soussou, PH.D.**[§], and **Huei-Sheng Vincent Chen, M.D., PH.D.**[*,#]

[*]Center for Neuroscience, Aging and Stem Cell Research, Sanford-Burnham Medical Research Institute, La Jolla, California, USA [†]Modeling & Simulation, Novartis Pharma AG, Basel, Switzerland [‡]Faculty of Kinesiology, University of Calgary, Canada [§]QUASAR Inc., San Diego, California [#]Division of Cardiology, University of California-San Diego, San Diego, California, USA

Abstract

Introduction—Understanding sinoatrial node (SAN) development could help in developing therapies for SAN dysfunction. However, electrophysiological investigation of SAN development remains difficult because mutant mice with SAN dysfunctions are frequently embryonically lethal. Most research on SAN development is therefore limited to immunocytochemical observations without comparable functional studies.

Methods and Results—We applied a multi-electrode array (MEA) recording system to study SAN development in mouse hearts acutely isolated at embryonic ages (E) 8.5 to 12.5 days. Physiological heart rates were routinely restored, enabling accurate functional assessment of SAN development. We found that dominant pacemaking activity originated from the left inflow tract (LIFT) region at E8.5, but switched to the right SAN by E12.5. Combining MEA recordings and pharmacological agents, we show that intracellular calcium (Ca^{2+})-mediated automaticity develops early and is the major mechanism of pulse generation in the LIFT of E8.5 hearts. Later in development at E12.5, sarcolemmal ion channels develop in the SAN at a time when pacemaker channels are down regulated in the LIFT, leading to a switch in the dominant pacemaker location. Additionally, low micromolar concentrations of tetrodotoxin (TTX), a sodium channel blocker, minimally affect pacemaker rhythm at E8.5–12.5; but suppress atrial activation and reveal a tetrodotoxin-resistant SAN-atrioventricular node (internodal) pathway that mediates internodal conduction in E12.5 hearts.

Conclusions—Using a physiological mapping method, we demonstrate that differential mechanistic development of automaticity between the left and right inflow tract regions confers the pacemaker location switch. Moreover, a tetrodotoxin-resistant pathway mediates preferential internodal conduction in E12.5 mouse hearts.

Correspondence: H.-S. Vincent Chen, M.D., Ph.D., Sanford-Burnham Medical Research Institute, 10901 North Torrey Pines Road, La Jolla, California 92037, USA. Tel: 858-646-3183; Fax: 858-795-5273; hsv_chen@burnham.org.

Author contributions

T. Yi and H.-S.V. Chen designed research; T. Yi, J. Wen, C. Kim and H.-S.V. Chen performed research; J. Wong and W. Soussou designed the software for activation map; S. Sink, O. Taghli-Lamallem and E. Feller contributed significantly to data analysis/interpretation; M. Fink provided motion analysis software; W. Giles evaluated and commented on the manuscript; T. Yi, and H.-S.V.C. wrote the paper.

Keywords

Electrophysiology mapping; Ion channel; Intracellular calcium; Sinoatrial node; Sinoventricular conduction; Internodal pathway

Introduction

Cardiac myocytes in the specialized cardiac conduction system display different electrical and immunocytochemical properties from surrounding working myocytes.[1, 2] Mouse models with genetic manipulations are frequently used to study embryonic development of cardiac conduction system, yet functional correlates are usually lacking. Also, physiological mechanisms underlying automaticity in mature sinoatrial node (SAN) cells remain controversial and most likely involve various sarcolemmal ion channels, ion exchangers, and intracellular Ca^{2+} cycling machinery.[2–5] Currently, the underlying mechanisms for functional development of automaticity in early pacemaking or SAN cells remains unclear. Recent research has just begun to unravel molecular pathways governing structural development of SAN.[2, 6–8] Elucidation of molecular pathways directing electrophysiological development of the SAN will help in the development of genetic and cell-based therapies for treating sinus node dysfunction.[9]

Physiological studies of whole embryonic mouse hearts are usually challenging because of their small size and fragility. Lack of specific SAN tracking markers,[10] especially at early embryonic stages, limits the interpretation of single cardiomyocyte-based studies. Moreover, mutant mice with defective SAN function are frequently embryonic-lethal and cannot be studied further.[11] Therefore, most electrophysiological studies of functional development of pacemaker or conducting cells in early embryonic hearts have used voltage- or Ca^{2+}-sensitive dyes and derived their results by optical mapping methods. These optical mapping studies reported that the earliest pacemaking activity in embryonic chick or rat hearts was usually found in the left sinoatrial primordium (termed LIFT in this manuscript); yet sometimes it originated in the right sinoatrial region.[12, 13] While optical mappings have provided valuable insights toward functional development of cardiac conduction system,[12–14] the dye-loading process required for optical mapping may affect electrophysiological properties of hearts[15] or slow down heart rates,[12,13] which could result in wandering pacemakers as observed in early studies.[12,13] It is also unlikely that embryonic hearts from mutant mice with defective SAN development could survive the harsh dye-loading process. Genetically targetable or encoded Ca^{2+} indicators have recently been developed to avoid harsh dye-loading processes,[16] yet their widespread applications remain to be demonstrated. Consequently, the mechanism underlying the switch of pacemaker location during early cardiogenesis remains to be elucidated. An electrophysiological recording method without any influence of foreign dyes may be the most physiological means to study SAN development during early cardiogenesis and should be complementary to various existing recording methods. Additionally, because most embryonic cardiomyocytes can generate automaticity,[17] a system that constantly monitors dominant pacemaker location is needed so as to prevent misleading conclusions from wandering pacemakers originating from working cardiomyocytes.

Here, we applied a multi-electrode array (MEA) recording system[18] with motion detection algorithms to determine the mechanism of switch in pacemaker location (referred to here as ‘pacemaker location switch’) and signal conduction between the SAN and atrioventricular node (AVN) during early cardiogenesis at the organ level.

Methods

Details of all protocols and antibodies used are provided in Online Supplements.

Isolation of Embryonic Mouse Heart

To establish an embryonic mouse heart preparation with physiological heart rhythm, pregnant mice (C57/B6) were sedated by repetitive i.p. injections of Avertin and ventilated with 95%O_2/5% CO_2 throughout the experimental period. Embryonic age of 0.5 day was designated at noon on the day a vaginal plug was detected after overnight mating. Individual embryos were dissected consecutively and embryonic hearts were then isolated with a dissecting microscope at room temperature. Isolated hearts were immediately recovered with 37°C pre-oxygenated Dulbecco's modified eagle medium (DMEM) to obtain optimal physiological functions.

MEA Recordings and Pharmacological Applications

Each acutely isolated embryonic heart was placed directly onto a MEA chamber containing 60 gold electrodes (10–30 μm electrode with 20–200 μm inter-electrode spacing, Supplemental Fig. 1). All experiments were conducted at 37°C, and MEA chamber was continuously perfused with pre-oxygenated (95% O_2/5% CO_2) DMEM containing 1.8 mmol/L Ca^{2+} with or without drugs (1–2 ml/min). Spontaneous field potentials were recorded at 10kHz by the MEA data acquisition system. The sources of pharmacological agents and their applications are detailed in Online Supplements (Supplemental Figs. 2–4). The dominant pacemaker regions during experiments were constantly monitored and a switch of pacemaker location was indicated when it occurred.

Video Imaging with Motion Detection Algorithm

For capturing the contraction sequence, each heart was imaged with a digital camera during electrophysiological recordings. The imaging data were analyzed with motion detection software provided by Dr. Martin Fink. Video imaging procedure and analysis are detailed in Online Supplement. Video imaging was also used to confirm that each electrode recorded from the same location of individual heart throughout each respective experiment (Supplemental Movie 1).

Immunohistochemistry of Frozen Heart Sections and In Situ Hybridization

Standard techniques were used for immunostaining, cryosections, and *in situ* hybridization of embryonic mouse hearts.

Statistical Analysis

Data are presented as the mean ± SD (standard deviation). Using the StatView program (SAS institute, NC), statistical differences were analyzed by an ANOVA procedure with post hoc Tukey/Kramer test for multiple comparisons. A statistical difference with a p-value < 0.05 was considered significant and was labeled with an asterisk (*) in all figures.

Results

Establishing a physiological mapping system to track the fate of embryonic dominant pacemaker sites

We applied the MEA recording system and video†imaging with a motion detection algorithm to analyze cardiac electrical activities and contractions of acutely isolated embryonic mouse hearts. MEA recordings of E8.5 (Fig. 1A) and E12.5 hearts (with dorsal SAN side contacting electrodes, Fig. 1B) are shown. Figures 1C–D depicts comparable field

potential electrograms from various recording electrodes of respective hearts. MEA recordings illustrated a single field potential propagating across various regions of E8.5 hearts yet revealed distinct SAN, atrial and ventricular signals in E12.5 hearts. Based on the activation sequence of field potentials from various regions of embryonic hearts, the earliest location of electrical activities (termed the dominant pacemaker site) could be determined. The local activation time (LAT) of various cardiac regions is determined by the midpoint of maximal negative slope of field potentials at each recording electrode (Fig. 1E).[19] At E12.5, when distinct signals with large amplitudes could be recorded, we can also transform respective local activation time of field potential signals from all electrodes to activation maps (similar to the activation map generated by the CARTO system in clinical cardiac electrophysiology)[20] for a graphic demonstration of myocardial activation sequence using MATLAB software (Fig. 1F). In Figure 1F (and Supplemental Movie 2), the earliest activation (red) at E12.5 was located at the right-sided SAN (SAN map) with bilateral atrial signal propagation (A map) and double apical ventricular breakthroughs (V map).[14] Video imaging with a motion detection algorithm is used in parallel to match the sidedness of earliest contraction to earliest electrical activation for confirming proper excitation-contraction coupling (Supplemental Fig. 5). This video imaging is especially useful at E8.5 when excessive manipulation of small hearts must be avoided due to their fragility. With our recording system, measured heart rates (HRs) from these isolated hearts are relatively stable for >30 minutes and are similar to measured *in vivo* HRs at comparable embryonic ages.[21] The initially restored HRs and stable HRs at 10 minutes (min) are: 121.6±29.2 and 108.9±28.0 beats per minute (bpm) at E8.5 (n=67); 160.0±25.5 and 142.4±26.4 bpm at E10.5 (n=29); as well as 180.6±23.5 and 171.3±21.6 bpm at E12.5 (n=81), respectively (Supplemental Fig. 2). Importantly, we found that earliest pacemaking activity always started from the LIFT region at E8.5 and generally switched to the right SAN area by E12.5 (pacemaker location switch) (Fig. 1G). The respective percentages of dominant right-sided pacemaker at E8.5, 10.5, and 12.5 are 0% (n=80), 64.1% (n=39), and 88.4% (n=95). In rare cases (~4%) when the signal quality of video imaging or MEA recording was poor, we cited the origin of the dominant pacemaker as "undetermined." Additionally, this MEA-based recording system allows efficient pharmacological investigation of pacemaking mechanisms during cardiogenesis at the organ level (see below).

Intracellular Ca^{2+} signaling is the major mechanism controlling automaticity of left-sided pacemaking cells located in the LIFT at E8.5

Since many mechanisms contribute to automaticity of pacemaker cells, we used the MEA system to simultaneously monitor locations and rate changes of dominant pacemaker sites by pharmacological blockers of ion channels or intracellular Ca^{2+} ($[Ca^{2+}]_i$) handling proteins to elucidate developmental changes in mechanisms controlling dominant automaticity during early cardiogenesis. Dense mapping of E8.5 hearts (Fig. 1A) was used to construct Figures 2–3.

The $[Ca^{2+}]_i$ handling machinery, including inositol 1,4,5-trisphosphate (IP3) receptor (IP_3R),[22] type 2 Ryanodine receptor (RyR2),[23] and type 1 sodium (Na^+)/ Ca^{2+} exchanger (NCX1),[3, 11] had been implicated in the generation of pacemaker rhythms in adult mouse SAN cells. We applied various antagonists to determine which of these $[Ca^{2+}]_i$ handling proteins contributed to automaticity at dominant pacemaker sites during early cardiogenesis. KB-R7943 (KB) at 50 μM is reported to significantly block outward current via NCX1 (the reverse mode) and modestly inhibit inward current through NCX1 (the forward mode).[24] In Figures 2A–C, application of 50 μM KB minimally affected HRs of E8.5 hearts (4.7±4.9% blockade, n=12) and decreased HRs from E12.5 SAN by only 14.2±4.3% (n=14). 10 μM Ryanodine, a RyR2 blocker,[25] decreased HRs of E8.5 (n=9) and E12.5 (n=16) hearts by 18.4±6.9% and 27.9±12.1% respectively. However, after Ryanodine or KB blockade, co-

application of 50 μM KB and 10 μM Ryanodine for 10 minutes completely abolished HRs originating from LIFT in all E8.5 hearts tested (Zero HR at LIFT, n=8). In 3 of 8 E8.5 hearts, residual pacemaking activity could be detected only at the right inflow tract (RIFT) region (mean residual HR at RIFT is 15.9±25.0%) with arrested LIFT automaticity after exposure to these two drugs (Fig. 2B bottom left). The remaining cardiac rhythm from RIFT in these 3 hearts was slow, irregular and eventually ceased to function if an additional 10-minute recording was performed, suggesting immature RIFT pacemakers. These results indicate that $[Ca^{2+}]_i$ signaling is the major mechanism controlling earliest left-sided automaticity in E8.5 hearts. Results in Figure 2C also showed that KB alone minimally affected HRs of E8.5 LIFT at baseline (<5% blockade) when Ryanodine receptors are fully functional, yet significantly blocked HRs (100% blockade) when Ryanodine receptors are deficient. This non-additive effect suggests that NCX1 acts as an automaticity reserve to compensate the loss of Ryanodine receptors (or vice versa) for maintaining cardiac rhythm at E8.5 LIFT. Also, this significant compensatory mechanism by various $[Ca^{2+}]_i$ handling apparatus at E8.5 may explain the small effect of single drug, either KB (4.7±4.9% blockade) or Ryanodine alone (18.4±6.9% blockade), on HRs originating from LIFT. In contrast, at E12.5, co-application of KB and Ryanodine decreased HRs of right-sided SAN by 45.0±9.9% (n=9, close to additive blockade from both drugs: 14.2%+27.9%=42.1%) and did not cause any pacemaker switch. Thus, although both Ryanodine receptor and NCX1 contributed to automaticity of SAN at E12.5, they did not compensate each other when one is deficient. Additionally, substantial residual heart rhythm (55±9.9%, n=9) remains after the combined blockade by KB and Ryanodine at E12.5. These results indicate additional mechanisms, such as ion channels, may play increasing contributions to the automaticity at E12.5.

Furthermore, 10 μM 2-APB (2-aminoethoxydiphenyl borate), a membrane-permeable IP_3R blocker,[26] minimally decreased HRs of E8.5 (n=7) and E12.5 (n=7) hearts (8% and 5% respectively, Fig. 2A, C). However, after RyR blockade, 10 μM 2-APB decreased HRs of E8.5 (n=8) and E12.5 (n=7) hearts by an additional 15% and 11% respectively (Fig. 2C), indicating that IP_3Rs also play a small part in automaticity reserve when Ryanodine receptors are deficient at both ages. Ratios of residual HRs relative to baseline HRs (mean ± SD in %) after drug blockade by these pharmacological agents during development are summarized in Figure 2C and its legend. The degree of HR blockade by two drugs in combination is always more than one drug alone (ANOVA, $p<0.05$) at either E8.5 or E12.5 (Fig. 2C). Each pairwise comparison is indicated by connecting lines with an asterisk denoting a p-value <0.05 (Fig. 2C). Of note, each drug used alone in this study did not produce similar effects on automaticity or field potential properties as other ion channel blockers or with respect to one another; rendering non-specific action from each drug unlikely.

Increasing contribution of sarcolemmal ion channels to automaticity control in right-sided SAN cells with faster heart rates at E12.5

Although $[Ca^{2+}]_i$ signaling plays a major role in generating automaticity at the LIFT of E8.5 hearts, the switch of dominant pacemaker site to the right-sided SAN (Fig. 1G) with a concomitant increase in pacemaker rates at E12.5 (Supplemental Fig. 2) suggests that additional mechanisms of automaticity may evolve with embryonic development. For instance, hyperpolarization-activated, cyclic nucleotide-gated (HCN) cation channels, especially the type 4 isoform (HCN4), are thought to mediate pacemaker activity of mature SAN cells.[4–5] ZD7288 at 1–10 μM is a specific HCN channel blocker and is used to inhibit HCN-mediated current (I_f) and automaticity.[27] We found that 10 μM ZD7288 blocked HRs of E8.5 hearts by 27.4±10.8% (n=20) and significantly reduced HRs of E12.5 hearts by 66.0±11.0% (n=15, Fig. 3A–B). Furthermore, T-type Ca^{2+} channels have also been

implicated in physiological and neurohormonal modulation of heart rates.[28] Mibefradil at 1 μM[29] and nickel at 40 μM[30] are relatively specific blockers for T-type Ca^{2+} channels. 1 μM Mibefradil slightly decreased HRs of E8.5 hearts by 9.4±8.0% (n=12) and significantly decreased HRs of E12.5 SANs by 28.3±7.5% (n=15, Fig. 3A–B). Nickel (40 μM) produced similar patterns of blockade on HRs as 0.5 μM Mibefradil (Supplemental Fig. 6A). Results of residual HRs (relative to baseline HRs) after exposure to HCN and T-type Ca^{2+} channel blockers are summarized in Figure 3B. Pairwise comparisons (indicated by connecting lines) between E8.5 and E12.5 groups after each drug treatment (ANOVA, with all *p*-values <0.01) in Fig. 3B demonstrate that sarcolemmal ion channels play increasing contributions to automaticity at E12.5 than at E8.5.

Immunostaining with HCN4 antibodies revealed more positive staining for HCN4 channels in LIFT than RIFT regions of E8.5 hearts (Supplemental Fig. 6B–C). HCN4 immunolabeling increased at the right SAN region and was down-regulated significantly in left atria of E12.5 hearts (right panel in Supplemental Fig. 6B, and Supplemental Fig.6C). Immunostaining with $Ca_V3.1$ and $Ca_V3.2$ antibodies, two main subunits for T-type Ca^{2+} channels, showed minimal presence of membrane T-type Ca^{2+} channel subunits in either LIFT or RIFT regions of E8.5 hearts (Supplemental Fig. 6Da–c). The $Ca_V3.1$ and $Ca_V3.2$ staining was up-regulated in both atria of E12.5 hearts and some $Ca_V3.1$/$Ca_V3.2$ staining could also be observed at the right SAN region (Supplemental Fig. 6Dd–f). These results suggest that sarcolemmal ion channels play an increasing role in generating “faster” pacemaker rhythm from E8.5 to E12.5, reflecting ongoing differentiation and/or maturation. This mechanistic maturation of automaticity appears to accompany the location switch of dominant pacemaker sites (Fig. 1G) during early cardiogenesis from E8.5 to E12.5.

The role of sodium channels in cardiac automaticity and propagation of E8.5 and E12.5 hearts

The relatively TTX-resistant cardiac isoform of sodium (Na^+) channels, $Na_V1.5$, and the TTX-sensitive neuronal isoform, $Na_V1.1$, have been suggested to underlie pacemaking and conduction of adult mouse SAN.[31] We used 2 μM TTX, which should block 100% of $Na_V1.1$ and at least >50% of $Na_V1.5$ channels, to determine the role of Na^+ channels in mediating dominant automaticity and cardiac conduction during early cardiogenesis.[31] 2 μM TTX minimally decreased HRs of E8.5 hearts (4.4±6.1%, n=7) and slightly prolonged field potential durations (FPDs) (9%, *p*=NS; Fig. 3C–F). In E12.5 hearts, MEA recordings clearly demonstrated SAN signals (Figs. 1 and 3), and the effect of TTX on SAN automaticity could be accurately evaluated. 2 μM TTX slightly reduced HRs of sinus rhythm (6.5±5.9%) at E12.5 (n=14) but significantly prolonged sinus node field potential duration (SNd, $p<0.01$ with ANOVA), sinoatrial conduction interval (SAI, $p<0.01$), and atrial field potential duration (AFPD, $p<0.01$) (Fig. 3F). 2 μM TTX also led to various degrees of sinoatrial (SA) exit blocks (Supplemental Fig. 7A) and RA-LA conduction block (Supplemental Fig. 7B). Prolongation of field potential duration and conduction interval without affecting HR suggests that Na^+ channels primarily contribute to electrical propagation and have minimal contribution to the dominant automaticity of E8.5 and E12.5 hearts. Values of residual HRs and various electrophysiological parameters (mean ± SD in %) after 2 μM TTX blockade are summarized in Figures 3D and F, respectively.

TTX revealed a functional inter-nodal conduction pathway in the RA of E12.5 hearts

Most importantly, 2 μM TTX revealed a TTX-resistant sino-ventricular conducting pathway in the RA without any atrial activation in 7 of 14 E12.5 hearts (Fig. 4A). Previous reports by Rentschler and colleagues demonstrated the existence of functional AVN-bundle branch-Purkinje axis for atrioventricular conduction and ventricular activation with earliest double breakthroughs at ventricular apex of E12.5 mouse hearts.[14] Color-coded activation maps

(Fig. 4B) demonstrated that the sequence of ventricular activation (double breakthroughs with apical-to-base propagation pattern) are the same between normally conducted beats with atrial activation (the first beat in Fig. 4A) and sino-ventricular (Sino-V) conduction without atrial excitation (the third beat in Fig. 4A), suggesting a preferential pathway mediating Sino-V conduction in the RA of E12.5 hearts from the SAN to ventricles via the AVN-Purkinje axis (Fig. 4B and see Supplemental Movies 3–5). The unchanged morphology of ventricular FPs in all ventricular leads (two representative leads are shown in Fig. 4C) and lack of any ventricular pre-excitation during Sino-V conduction also support that this preferential pathway connects the SAN to AVN conduction axis. Furthermore, during a stable 2:1 Sino-V conduction rhythm (Fig. 5A–B), changes of ventricular intervals (V1V1) followed the changes of preceding SAN signal intervals (S1S1) in a 1:1 relationship during both normal (S-A-V) and Sino-V conducted beats (Fig. 5B–C); suggesting ventricular activations were guided by the preceding SAN rhythm (SAN-V linking). Also, SAN signals detected from electrodes surrounding the SAN area demonstrated a high-SAN-to-low-SAN (high-to-low) conducting sequence during normal and Sino-V conducted beats (Fig. 5D–E). Thus, high-to-low SAN conducting sequences with persistent SAN-V linking ruled out the possibility of coincidental junctional escape beats during the Sino-V conduction. Moreover, during TTX blockade, two of the E12.5 hearts displayed short periods of sinus arrhythmia with wide ranges of sinus cycle-length (S1S1) variations, which enabled the assessment of responses of Sino-V intervals (SVI) during Sino-V conduction to preceding sinus cycle length (S1S1). The Sino-V intervals demonstrated decremental AVN conducting properties (Fig. 5F),[32] strongly supporting that a TTX-resistant internodal pathway mediates these Sino-V conducted beats.

The most plausible explanation for this TTX-resistant pathway is that the internodal pathway does not express nor relies on cardiac Na^+ channel subunits (mainly $Na_V1.5$) for signal propagation. Using $Na_V1.5$ antibodies, we found that an internodal pathway with very low $Na_V1.5$ expression indeed existed at the junction of RA and right sinus horn (rsh) at E12.5. Furthermore, with both HCN4 antibody labeling and *in situ* hybridization,[33] we found that this internodal pathway completely coincided with cells stained positive for HCN4 channels in the RA of E12.5 hearts (Fig. 6A–B). Using different markers for the cardiac conduction system (such as Tbx3 and Podoplanin), other groups also demonstrated a similar immunocytochemical distinct pathway in E12.5 mouse hearts connecting SAN to the AVN.[2,7] To the best of our knowledge, this study is the first electrophysiological demonstration of a functional and TTX-resistant pathway mediating internodal conduction in E12.5 mouse hearts.

Discussion

We applied a MEA-based electrophysiological mapping system that enables rapid restoration of physiological HRs, thereby allowing accurate functional assessment of early pacemaker development and pharmacological investigations. No foreign dyes were used so as to avoid any non-physiological influence on the properties of dominant pacemaker cells. Importantly, a distinct SAN signal could be consistently recorded in E12.5 mouse hearts, which enables accurate determination of automaticity mechanisms in the SAN at E12.5. We find that pacemaker dominance in mice switches from the LIFT at E8.5 to the right-sided SAN region by E12.5. Intracellular Ca^{2+} handling proteins develop early in the LIFT at E8.5, which dominates the control of automaticity. At later developmental stages when heart rates increase, sarcolemmal ion channels evolve in the SAN to play increasing roles in faster impulse generation. Furthermore, this mechanistic maturation of SAN automaticity, combined with concomitant ion channel down-regulation at the LIFT, confers the pacemaker location switch and permits faster responses to rising electrophysiological and neurohormonal demands (summarized in Fig. 6C). With pharmacological manipulations, a

clear pacemaker location switch could be demonstrated (Fig. 2B), suggesting the existence of two pacemaking regions as early as E8.5 with different degrees of maturation and mechanisms of impulse generation. Previously, Kamino's group used a "rhythmicity gradient" to explain the switch in dominant pacemaker locations in early cardiogenesis, yet provided no mechanistic insight.[12] In contrast, we show here that the pacemaker location switch during early cardiogenesis is the result of differential maturation of pacemaking mechanisms between the left and right inflow tract regions. Moreover, loss of left-sided dominance of automaticity coincides with down-regulation of HCN4 channels, suggesting inhibitory signals exist at LIFT area during cardiac development.[8]

Automaticity reserve develops early in cardiogenesis

Importantly, we find that compensatory mechanisms become operational as early as E8.5 to maintain heart rates and sustain lives when the dominant pacemaking mechanism is impaired. We show that a Ryanodine receptor or NCX blocker alone only slightly affects baseline heart rates at E8.5. However, small heart rate changes by a single blocker is likely due to compensatory mechanisms from additional $[Ca^{2+}]_i$ handling proteins because co-application of two blockers abolishes left-sided pacemaker and causes the pacemaker location switch (Fig. 2B–C).

Furthermore, mechanisms underlying automaticity become increasingly complex with further cardiac development. Ion channels, such as HCN and T-type Ca^{2+} channels, play increasing contributions to dominant automaticity of the SAN when heart rate becomes faster at E12.5. It is not possible to report the contribution of every ion channels to automaticity development in a single study. Therefore, future studies are needed to see if other ion channels also display increasing contributions to automaticity with cardiac development. Voltage-dependent ion channels could alter membrane potential faster than $[Ca^{2+}]_i$ handling machineries, and their increasing roles in mediating automaticity at E12.5 might be essential for developing faster heart rates to match rising metabolic demands. Nonetheless, we find that intracellular Ca^{2+}-mediated automaticity remains functional at E12.5, suggesting many mechanisms work together to play the fail-safe task in maintaining automaticity (automaticity reserve) at later stages of cardiac development. Also, because most embryonic cardiomyocytes exhibit automaticity,[17] our study indicates that simply evaluating heart rate changes by genetic manipulations or drug applications,[3–5,22,23,28] without monitoring locations of dominant pacemakers, might lead to erroneous interpretations about mechanisms of dominant automaticity during early embryonic development.

Existence of an embryonic internodal conduction pathway

Furthermore, using TTX, we find that Na^+ channels play a minor role in automaticity and contribute mainly to electrical propagation of E8.5-E12.5 mouse hearts. Most importantly, TTX treatment at low micromolar concentrations blocked atrial activation and revealed a TTX-resistant internodal conducting pathway in E12.5 hearts. This preferential pathway is consistent with immunocytochemical evidence shown by others using podoplanin and Tbx3 as cardiac conduction system markers.[2,7] Here, we provided the first functional evidence that such an internodal conduction pathway exists at the junction of RA/right sinus horn myocardium of E12.5 mouse hearts. However, this internodal pathway may not exist after birth since HCN4 immunostaining disappears at this internodal location in postnatal mouse hearts.[33]

Finally, this MEA-based recording technique is easy to perform, consistently enables the restoration of physiological heart rates, and facilitates pharmacological investigation of embryonic mouse hearts. This technique also reveals clear SAN signals for accurate

electrophysiological studies and therefore could complement various optical imaging methods. In the future, this method may potentially be applied to study SAN development of mutant mice that survive to E12.5 but could not tolerate the optical dye-loading process.

Supplementary Material

Refer to Web version on PubMed Central for supplementary material.

Acknowledgments

None.

Financial Support: Dr. Chen is supported by an Early Career Development Award from American College of Cardiology Foundation, and research grants from Bechtel Trusts & Foundation, California Institute of Regenerative Medicine (CIRM) (RS1-00171-1, RT1-01143, and RB2-01512), and NIH (HL105194)

REFERENCES

1. Schram G, Pourrier M, Melnyk P, Nattel S. Differential Distribution of Cardiac Ion Channel Expression as a Basis for Regional Specialization in Electrical Function. Circ Res. 2002; 90:939–950. [PubMed: 12016259]
2. Dobrzynski H, Boyett MR, Anderson RH. New insights into pacemaker activity: promoting understanding of sick sinus syndrome. Circulation. 2007; 115:1921–1932. [PubMed: 17420362]
3. Lakatta EG, Vinogradova T, Lyashkov A, Sirenko S, Zhu W, Ruknudin A, Maltsev VA. The integration of spontaneous intracellular Ca^{2+} cycling and surface membrane ion channel activation entrains normal automaticity in cells of the heart's pacemaker. Ann N Y Acad Sci. 2006; 1080:178–206. [PubMed: 17132784]
4. Barbuti A, DiFrancesco D. Control of cardiac rate by "funny" channels in health and disease. Ann N Y Acad Sci. 2008; 1123:213–223. [PubMed: 18375593]
5. Irisawa H, Brown HF, Giles W. Cardiac pacemaking in the sinoatrial node. Physiol Rev. 1993; 73:197–227. [PubMed: 8380502]
6. Wiese C, Grieskamp T, Airik R, Mommersteeg MT, Gardiwal A, de Gier-de Vries C, Schuster-Gossler K, Moorman AF, Kispert A, Christoffels VM. Formation of the sinus node head and differentiation of sinus node myocardium are independently regulated by Tbx18 and Tbx3. Circ Res. 2009; 104:388–397. [PubMed: 19096026]
7. Gittenberger-de Groot AC, Mahtab EA, Hahurij ND, Wisse LJ, Deruiter MC, Wijffels MC, Poelmann RE. Nkx2.5-negative myocardium of the posterior heart field and its correlation with podoplanin expression in cells from the developing cardiac pacemaking and conduction system. Anat Rec. 2007; 290:115–122.
8. Wang J, Klysik E, Sood S, Johnson RL, Wehrens XH, Martin JF. Pitx2 prevents susceptibility to atrial arrhythmias by inhibiting left-sided pacemaker specification. Proc Natl Acad Sci. 2010; 107:9753–9758. [PubMed: 20457925]
9. Rosen MR, Brink PR, Cohen IS, Robinson RB. Genes, stem cells and biological pacemakers. Cardiovasc Res. 2004; 64:12–23. [PubMed: 15364609]
10. Viswanathan S, Burch JB, Fishman GI, Moskowitz IP, Benson DW. Characterization of sinoatrial node in four conduction system marker mice. J Mol Cell Cardiol. 2007; 42:946–953. [PubMed: 17459410]
11. Conway SJ, Kruzynska-Frejtag A, Wang J, Rogers R, Kneer PL, Chen H, Creazzo T, Menick DR, Koushik SV. Role of sodium-calcium exchanger (Ncx1) in embryonic heart development: a transgenic rescue? Ann N Y Acad Sci. 2002; 976:268–281. [PubMed: 12502569]
12. Kamino K. Optical Approaches to Ontogeny of electrical activity and related functional organization during early heart development. Physiol Rev. 1991; 71:53–91. [PubMed: 1986392]
13. Hirota A, Kamino K, Komuro H, Sakai T, Yada T. Early events in development of electrical activity and contraction in embryonic rat heart assessed by optical recording. J Physiol. 1985; 369:209–227. [PubMed: 4093880]

14. Rentschler S, Vaidya DM, Tamaddon H, Degenhardt K, Sassoon D, Morley GE, Jalife J, Fishman GI. Visualization and functional characterization of the developing murine cardiac conduction system. Development. 2001; 128:1785–1792. [PubMed: 11311159]
15. Nygren A, Kondo C, Clark RB, Giles WR. Voltage-sensitive dye mapping in Langendorff-perfused rat hearts. Am J Physiol Heart Circ Physiol. 2003; 284:H892–H902. [PubMed: 12424095]
16. Palmer AE, Tsien RY. Measuring calcium signaling using genetically targetable fluorescent indicators. Nat Protoc. 2006; 1:1057–1065. [PubMed: 17406387]
17. Van Mierop LH. Location of pacemaker in chick embryo heart at the time of initiation of heartbeat. Am J Physiol. 1967; 212:407–415. [PubMed: 6018026]
18. Reppel M, Pillekamp F, Lu ZJ, Halbach M, Brockmeier K, Fleischmann BK, Hescheler J. Microelectrode arrays: a new tool to measure embryonic heart activity. J Electrocardiol. 2004; 37(Suppl):104–109. [PubMed: 15534818]
19. Chuck ET, Freeman DM, Watanabe M, Rosenbaum DS. Changing activation sequence in the embryonic chick heart: implications for the development of the His-Purkinje system. Circ Res. 1997; 81:470–476. [PubMed: 9314827]
20. Gepstein L, Hayam G, Ben-Haim SA. A novel method for nonfluoroscopic catheter-based electroanatomical mapping of the heart: in vitro and in vivo accuracy results. Circulation. 1997; 95:1611–1622. [PubMed: 9118532]
21. Mai W, Le Floc'h J, Vray D, Samarut J, Barthez P, Janier M. Evaluation of cardiovascular flow characteristics in the 129Sv mouse fetus using color-Doppler-guided spectral Doppler ultrasound. Vet Radiol Ultrasound. 2004; 45:568–573. [PubMed: 15605851]
22. Méry A, Aimond F, Ménard C, Mikoshiba K, Michalak M, Pucéat M. Initiation of embryonic cardiac pacemaker activity by inositol 1,4,5-trisphosphate-dependent calcium signaling. Mol Biol Cell. 2005; 16:2414–2423. [PubMed: 15758029]
23. Boheler KR, Czyz J, Tweedie D, Yang HT, Anisimov SV, Wobus AM. Differentiation of pluripotent embryonic stem cells into cardiomyocytes. Circ Res. 2002; 91:189–201. [PubMed: 12169644]
24. Watanabe Y, Koide Y, Kimura J. Topics on the Na^+/Ca^{2+} exchanger: pharmacological characterization of Na^+/Ca^{2+} exchanger inhibitors. J Pharmacol Sci. 2006; 102:7–16. [PubMed: 16990699]
25. Sutko JL, Airey JA, Welch W, Ruest L. The pharmacology of ryanodine and related compounds. Pharmacol Rev. 1997; 49:53–98. [PubMed: 9085309]
26. Gysembergh A, Lemaire S, Piot C, Sportouch C, Richard S, Kloner RA, Przyklenk K. Pharmacological manipulation of Ins(1,4,5)P3 signaling mimics preconditioning in rabbit heart. Am J Physiol. 1999; 277:H2458–H2469. [PubMed: 10600869]
27. Briggs I, BoSmith RE, Heapy CG. Effects of Zeneca ZD7288 in comparison with alinidine and UL-FS 49 on guinea pig sinoatrial node and ventricular action potentials. J Cardiovasc Pharmacol. 1994; 24:380–387. [PubMed: 7528293]
28. Mangoni ME, Couette B, Marger L, Bourinet E, Striessnig J, Nargeot J. Voltage-dependent calcium channels and cardiac pacemaker activity: from ionic currents to genes. Prog Biophys Mol Biol. 2006; 90:38–63. [PubMed: 15979127]
29. Clozel JP, Ertel EA, Ertel SI. Discovery and main pharmacological properties of mibefradil (Ro 40-5967), the first selective T-type calcium channel blocker. J Hypertens. 1997; 15:S17–S25.
30. Ono K, Iijima T. Pathophysiological significance of T-type Ca^{2+} channels: properties and functional roles of T-type Ca^{2+} channels in cardiac pacemaking. J Pharmacol Sci. 2005; 99:197–204. [PubMed: 16272791]
31. Lei M, Jones SA, Liu J, Lancaster MK, Fung SS, Dobrzynski H, Camelliti P, Maier SK, Noble D, Boyett MR. Requirement of neuronal- and cardiac-type sodium channels for murine sinoatrial node pacemaking. J Physiol. 2004; 559:835–848. [PubMed: 15254155]
32. Josephson, ME. Electrophysiological Investigation. 3rd ed.. Josephson, ME., editor. Boston, Mass: Kluwer; 2002. p. 19-67.Clinical Cardiac Electrophysiology.

33. Garcia-Frigola C, Shi Y, Evans SM. Expression of the hyperpolarization-activated cyclic nucleotide-gated cation channel HCN4 during mouse heart development. Gene Expr Patterns. 2003; 3:777–783. [PubMed: 14643687]

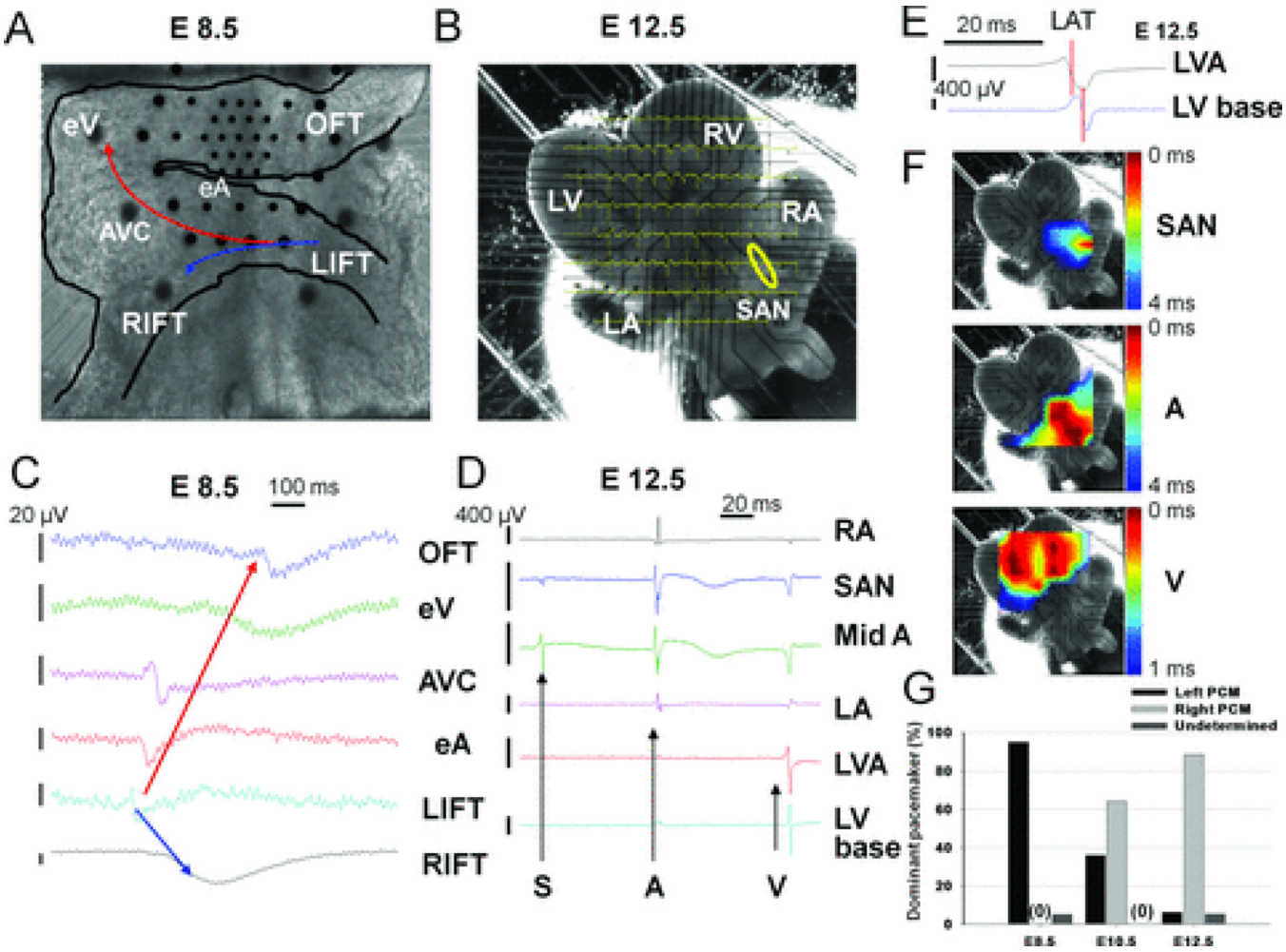

Figure 1. MEA-based electrophysiological mapping of embryonic mouse hearts

A: Image of an E8.5 heart with a dense Hexa array (Supplemental Fig. 1). B: Image of an E12.5 heart with a standard 30 × 200 μm array. The yellow circle indicates SAN. C: Field potentials (FPs) recorded from external cardiac surface of the E8.5 heart in A. The arrows (red or blue) indicate the sequence of activation from the dominant pacemaker site at the LIFT. D: FPs from B. Black arrows indicate the distinct sinal (S), atrial (A) and ventricular (V) signals respectively in the E12.5 heart. E: The method to determine LAT (labeled with a red vertical bar) is explained in Text. F: Activation maps of SAN, bilateral atria (A), and bilateral ventricles (V) demonstrate electrical propagation sequences (red is early and blue is late). G: Summary of the locations of dominant pacemakers, determined by both MEA and video recordings, at E8.5, E10.5 and E12.5 is shown. RIFT and LIFT indicate right and left inflow tract; eA and eV, embryonic atrium and ventricle; AVC, atrioventricular canal; RA and LA, right and left atrium; RV and LV, right and left ventricle; OFT, outflow tract; LVA, LV apex. Vertical bars represent the amplitudes of FP voltage and horizontal bars, time.

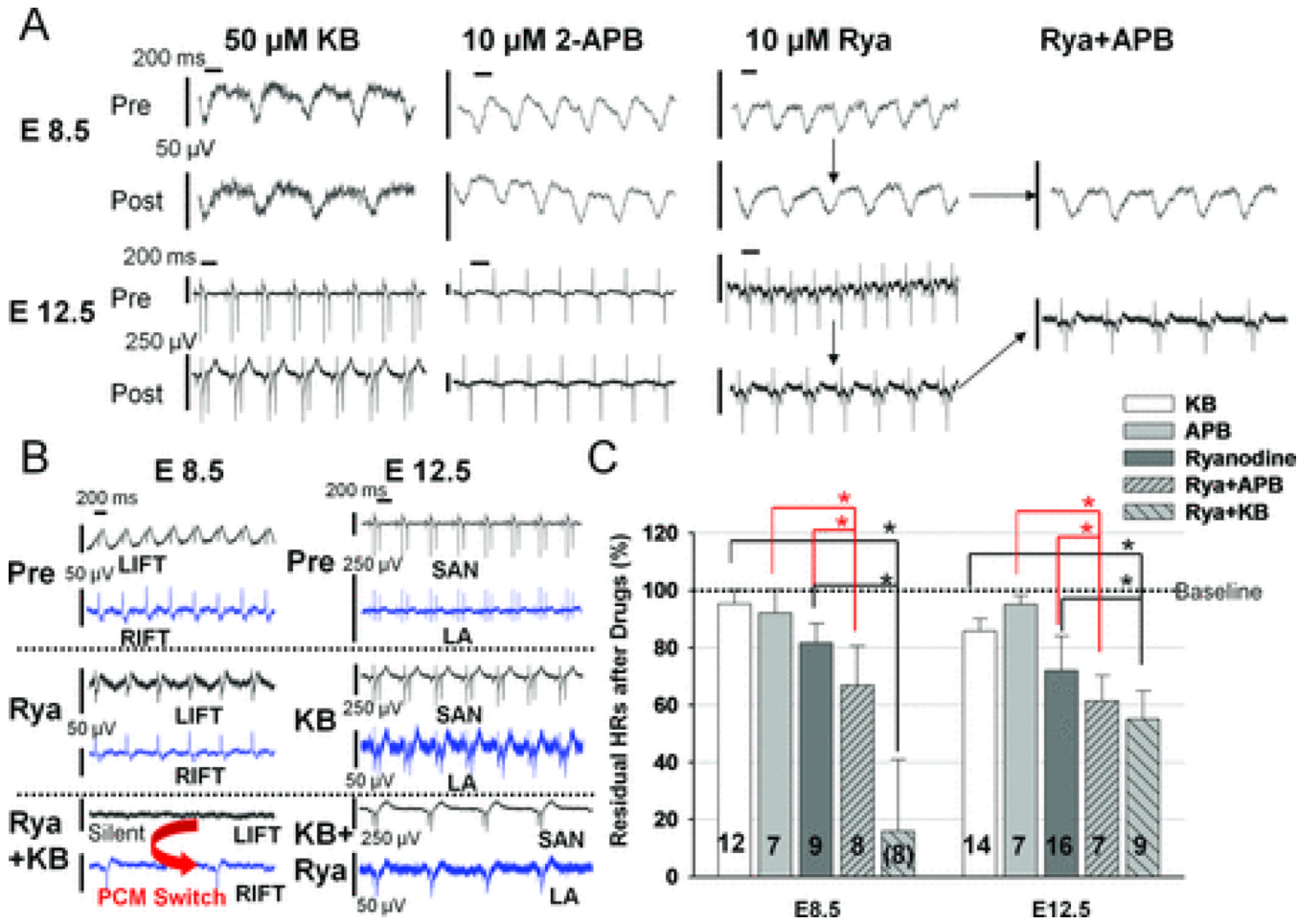

Figure 2. Intracellular Ca^{2+} handling proteins control the dominant automaticity of E8.5 hearts

A: Raw MEA tracings from the LIFT of E8.5 hearts and from the SAN of E12.5 hearts at baseline (Pre; before drug application) and 10 minutes after drug application (Post) are shown. B: Raw tracings from left and right pacemaker sites are shown to illustrate the effect on HRs by co-application of Ryanodine (Rya) and KB after either Rya (E8.5) or KB (E12.5) blockade. At E8.5, combination of Rya and KB completely arrested LIFT pacemaking activity in all hearts, and 3 of 8 hearts displayed residual pacemaker activity in the RIFT (pacemaker location switch, left bottom tracing). C: Summary of effects of 10 Rya, 50 KB, and 10 APB (in μM) on HRs of E8.5 and E12.5 hearts. Values of residual HRs after drugs relative to controls in this histogram for E8.5 and E12.5 hearts are: KB: 95.3±4.9 and 85.8±4.3%; APB: 92.1±8.1 and 95.2±3.0%; Rya: 81.6±6.9 and 72.1±12.1%; Rya+APB: 67.0±13.7 and 61.5±8.8%; and Rya+KB: 15.9±25.0 and 55.0±9.9%, respectively. Asterisks indicate $p<0.05$. The number in each column represents the number of hearts tested. Vertical bars represent 50 μV at E8.5 and 250 μV at E12.5 hearts in this and following figures unless otherwise indicated. Horizontal bars denote 200 ms.

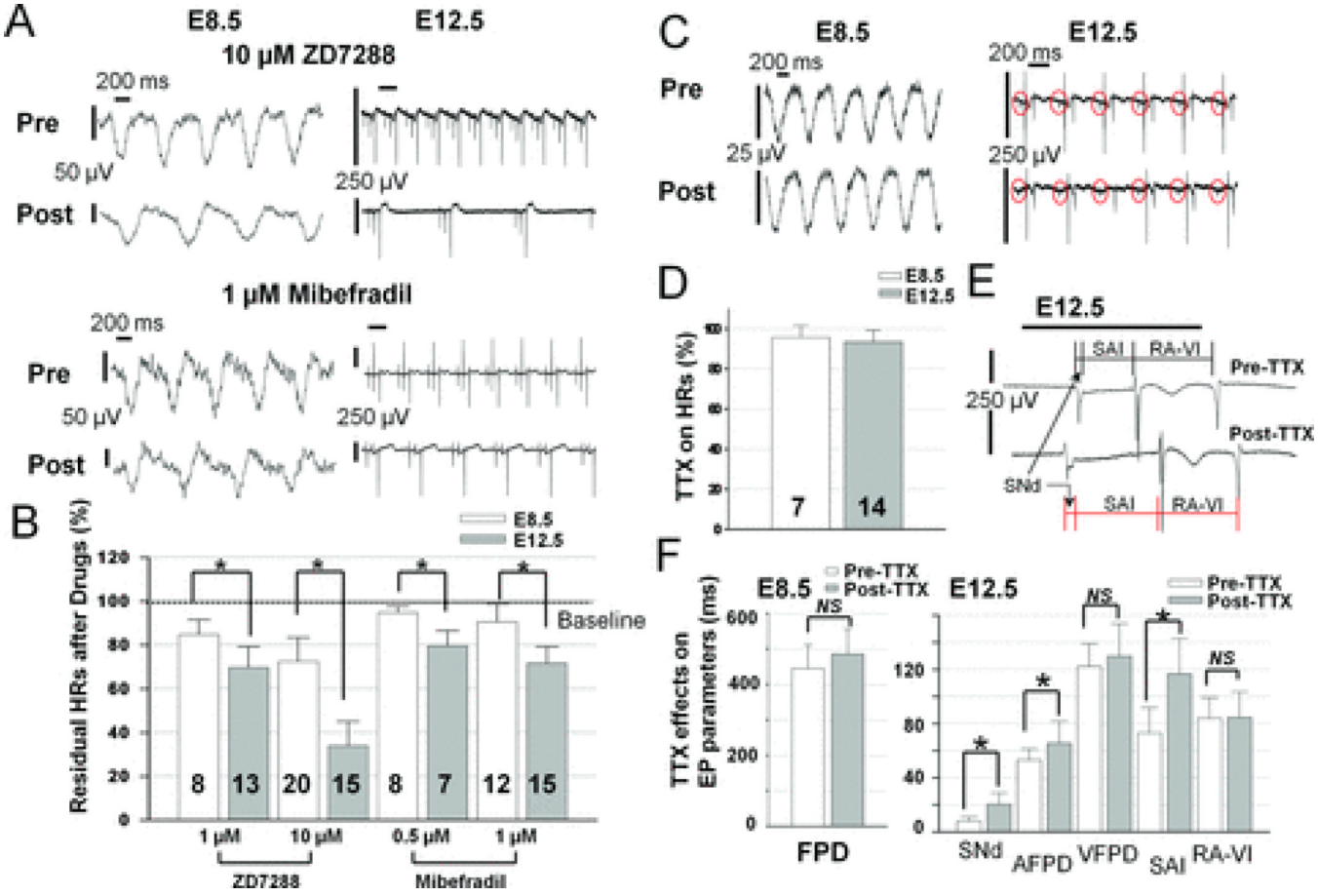

Figure 3. HCN and T-type Ca^{2+} channels, but not Na^{+} channels, play increasing roles in dominant automaticity with cardiac differentiation

A: Raw MEA tracings from the LIFT of E8.5 hearts and from the SAN of E12.5 hearts at baseline (Pre) and after drug application (Post) are shown. ZD7288 (top) and Mibefradil (bottom) reduced HRs of E12.5 hearts much more than E8.5 hearts. B: Summary of effects of ZD7288 and Mibefradil on heart rates. Values of residual HRs after drugs (in μM) in this histogram for E8.5 and E12.5 hearts are 1 ZD: 84.7±6.7 and 69.8±9.4%; 10 ZD, 72.6±10.8 and 34.0±11.0%; 0.5 Mibefradil, 94.8±2.7 and 79.5±7.0%; 1 Mibefradil, 90.6±8.0% and 71.7±7.5% respectively. Asterisks indicate difference between E8.5 and E12.5 with $p<0.01$ in this figure. C: Raw MEA tracings from the LIFT of E8.5 hearts (left) and from the SAN of E12.5 hearts (middle) at baseline (Pre) and after TTX application (Post) are shown. Red circles indicate sinus signals. D: TTX minimally decreased HRs of E8.5 (n= 7) and E12.5 (n=14) hearts to 95.6±6.1% and 93.5±5.9% of controls respectively. E: Schematic demonstration of the measurement of sinus field potential duration (SNd), sinoatrial interval (SAI), and RA to ventricular interval (RA-VI) pre and post TTX application. F: Summary of TTX effects on electrophysiological properties of E8.5 and E12.5 hearts. TTX slightly prolonged field potential durations (FPDs) at E8.5 (left, 444.5±66.5 vs. 485.3±70.5 ms, p=NS). At E12.5, TTX significantly prolonged SNd, atrial field potential duration (AFPD) and SAI (7.9±3.2 vs. 20.4±8.3, 53.2±8.2 vs. 65.7±16.2, and 73.2±18.6 vs. 116.7±26.2 ms, respectively) with minimal effects on ventricular field potential duration (VFPD, 122.2±16.9 vs. 129.8±24.0 ms) and RA-VI (84.0±15.3 vs. 84.7±18.8 ms). Asterisks indicate a difference between pre and post TTX with p-values <0.01 in Fig. 3F. *NS* indicates no significant difference between comparisons (ANOVA).

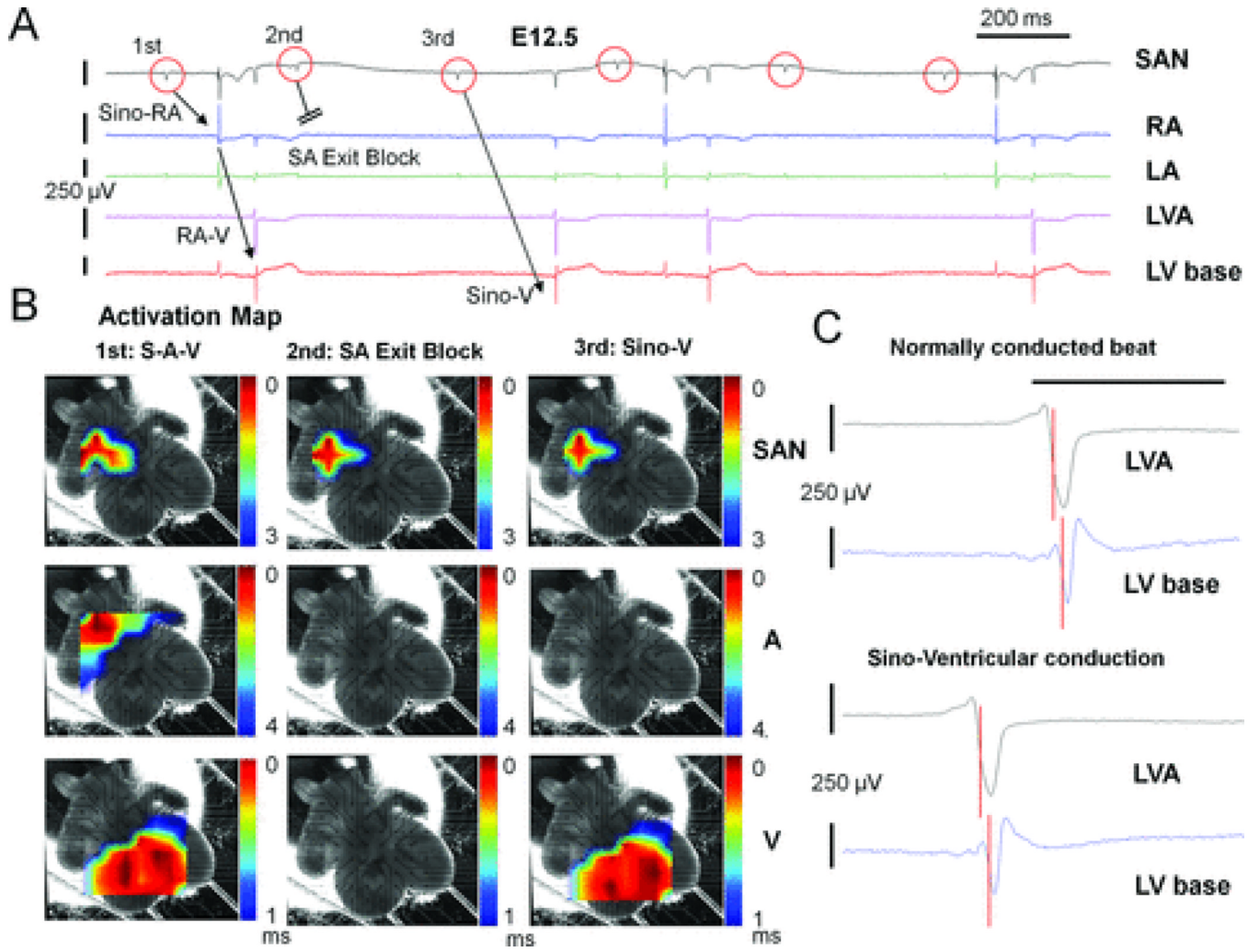

Figure 4. TTX revealed a preferential conduction pathway in the RA of E12.5 hearts

A: Raw MEA tracings of an E12.5 heart after TTX application are shown. TTX led to normal sino-atrial-ventricular activation (S-A-V) sequence (1st beat), complete sinoatrial (SA) exit block (2nd beat), and Sino-V conduction without atrial activation (3rd beat). B: Activation maps of these three beats are shown here to demonstrate that the activation sequence of both ventricles is unchanged during Sino-V conduction. Pre-TTX baseline activation maps of this heart are shown in Fig. 1F. C: The morphologies of ventricular field potentials during Sino-V conduction (3rd beat) at LA apex (LVA) and LV base display no pre-excitation and are unchanged from a normally conducted beat (1st beat). The local activation time (LAT) at each location is labeled with a red vertical bar. The LV apex is activated earlier than LV base in both cases.

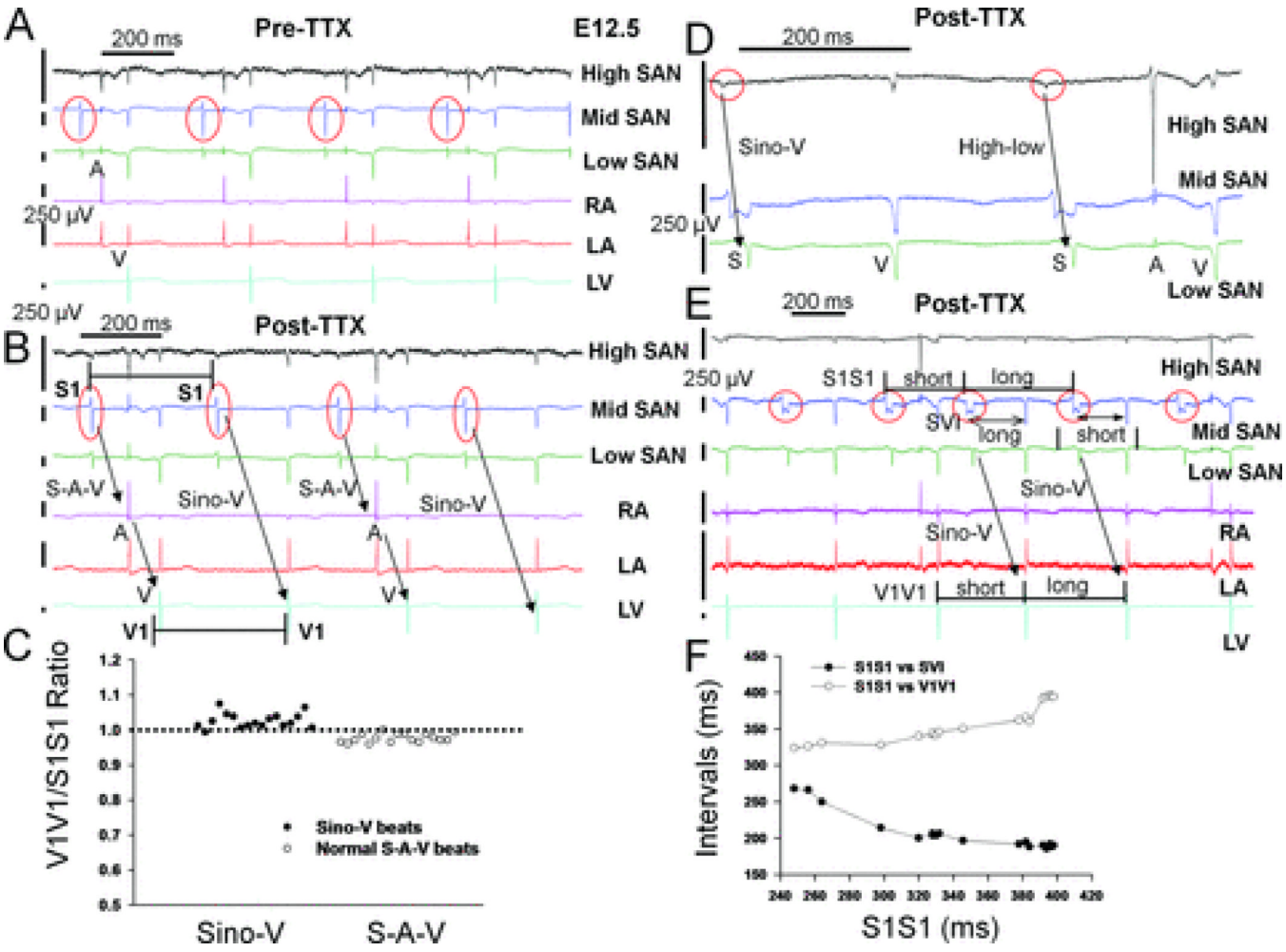

Figure 5. Sino-ventricular linking during Sino-V conduction and evidence for internodal conducting pathways

A: Raw MEA tracings from an E12.5 heart before and B: after TTX application. Electrical recordings from three consecutive electrodes around the SAN region and at a cranial-to-caudal sequence were named high, mid, or low SAN tracings in this figure (see also Supplements Fig. 3). TTX led to a stable pattern of alternating (2:1) normal sino-atrial-ventricular (S-A-V) (first and third beats) and Sino-V conduction sequences (second and fourth beats). C: During 12 sec recordings of stable 2:1 Sino-V conduction rhythm, the ratio of ventricular intervals (V1V1) to preceding sinus cycle length (S1S1) is close to 1 for all normal (S-A-V) and Sino-V conducted beats, indicating SAN-V linking. D: For another E12.5 heart with sinus arrhythmias, the high-to-low conducting sequence remains the same between normal and Sino-V conducted beats, as well as E, the sino-ventricular interval (SVI) during Sino-V conduction is longer after a short preceding S1S1 interval. F: Using all Sino-V conducted beats from a 30 sec recording period shown in E, a plot of V1V1 intervals and SVIs versus preceding S1S1 intervals showed a progressive increase in SVIs when S1S1 intervals were shorter than 320 ms, which is a classic decremental conduction property of AVN and supports an inter-nodal pathway that mediates Sino-V conduction with AVN as the relay. Red circles indicate sinus signals.

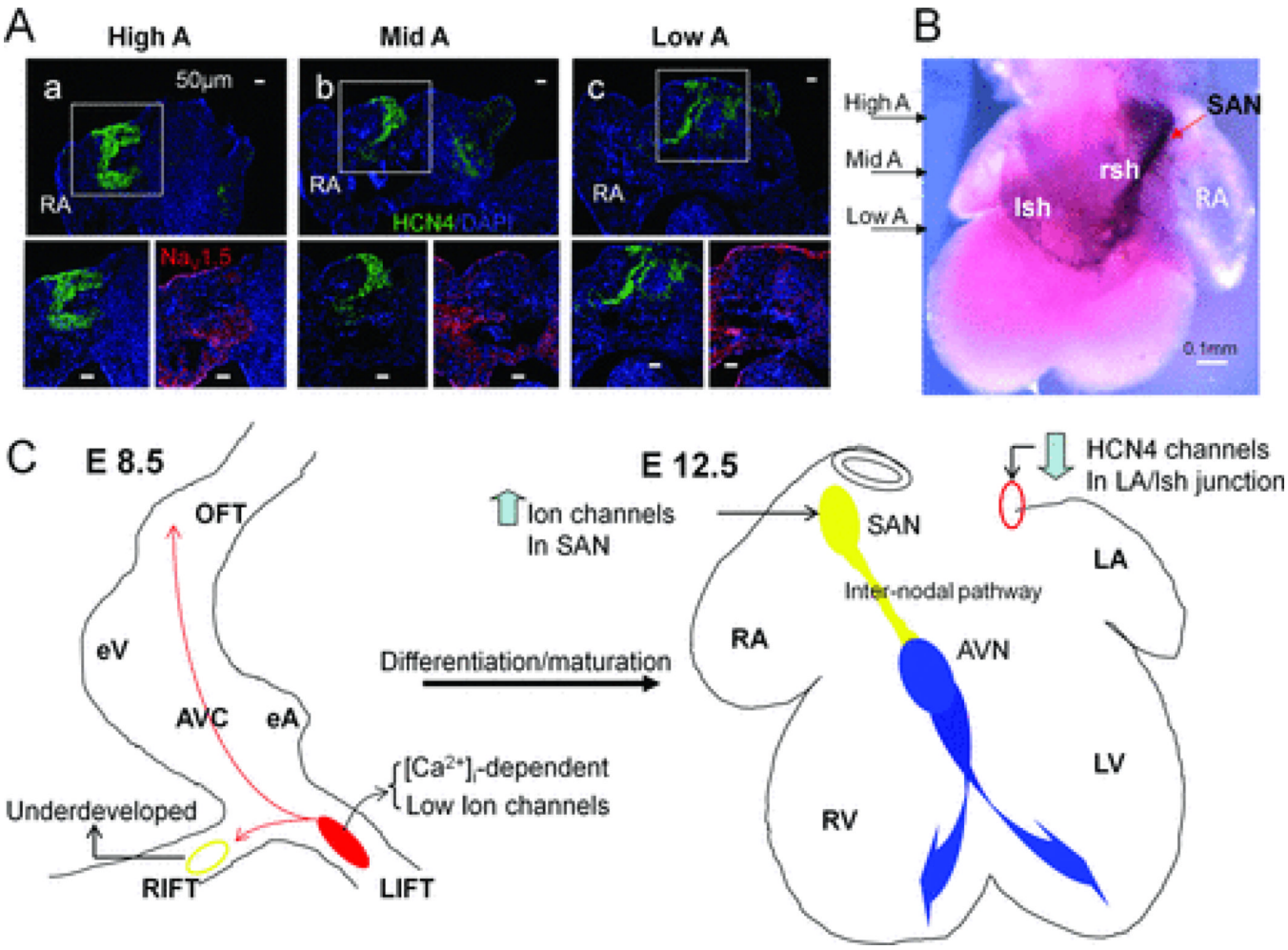

Figure 6. Immunostaining and *In situ* hybridization of HCN4 channels subunits revealed a potential internodal pathway at E12.5

A: Consecutive sections of E12.5 atria from high to low levels were obtained for immunostaining (only three levels of sections are shown here). Immunostainings of high atria (High A) at SAN level, middle atria (Mid A) and low atrial (Low A) close to AVN level are shown. Magnified views at each level showed a pathway throughout these atrial levels with high HCN4 staining (lower left) and low $Na_V1.5$ expression (lower right) at the RA-right sinus horn (rsh) junction. B: *In situ* hybridization (dorsal view) is used to show a continuous HCN4 expression pathway in the RA with arrows indicating comparable levels shown in A. C: Schematic summary of location and mechanistic switch of dominant automaticity during cardiac differentiation. Left panel, in E8.5 hearts, intracellular Ca^{2+}-driven mechanisms dominate control of the LIFT pacemaker site (red region) with small contributions of sarcolemmal ion channels to automaticity and an underdeveloped RIFT pacemaker site (yellow circle). Right panel, in E12.5 hearts, ion channels up-regulate (an arrow pointing up) in the right-sided SAN (filled yellow circle) and control the dominant rhythm with concomitant down-regulation (an arrow pointing down) of HCN4 channels in the comparable region at LA/ left sinus horn junction (red circle). An internodal conduction pathway (a yellow tract) could be demonstrated functionally in E12.5 hearts. The normal AVN-bundle branch-Purkinje system is labeled with blue color.